Materials Science and Engineering A 528 (2011) 5908–5913

Contents lists available at ScienceDirect

Materials Science and Engineering A

journal homepage: www.elsevier.com/locate/msea

Strain rate sensitivity of unequal grained nano-multilayers

P. Huang[a], F. Wang[b,*], M. Xu[a], T.J. Lu[b], K.W. Xu[a]

[a] State-key Laboratory for Mechanical Behavior of Material, Xi'an Jiaotong University, Xi'an 710049, People's Republic of China
[b] MOE Key Laboratory for Strength and Vibration, School of Aerospace, Xi'an Jiaotong University, Xi'an 710049, People's Republic of China

ARTICLE INFO

Article history:
Received 7 December 2010
Received in revised form 29 March 2011
Accepted 7 April 2011
Available online 13 April 2011

Keywords:
Multilayer
Strain rate sensitivity
Nanoindentation
Grain size
Grain boundary

ABSTRACT

Nanoscaled bimetallic Cu/Ta multilayers were fabricated and their deformation behaviors characterized under nanoindentation. The individual Cu and Ta layers had equal thickness (~30 nm) but quite different grain sizes. By evaluating the hardness of the bi-metal system at various strain rates, a transitional point of its strain rate sensitivity at the strain rate of 10^{-3} s^{-1} was observed. Contributions from dislocation and grain boundary (GB) motions to plastic deformation are found to be strongly dependent upon strain rate as well as grain size in alternative constituent layers. Whilst dislocation-mediated motions take up the majority of deformation in a Cu/Ta multilayer at high strain rates, GB motions occurring mainly in the Ta layers take over at low strain rates.

1. Introduction

Whilst the deformation behaviors of metallic nano-multilayers have been studied extensively, the focus has been mainly placed on bi-metallic systems having equal individual layer thickness [1–6]. As the grain size in an individual layer was in general implicitly assumed to be equal to its layer thickness, the bilayer thickness was considered as the sole parameter when evaluating the mechanical properties of the system. However, in practice, the grain size is not always equal to the individual layer thickness and, under certain circumstances, the effects of grain size on the mechanical properties of nano-multilayers cannot be neglected.

The plastic deformation mechanism of polycrystalline metals is typically grain size dependent, and the transition of deformation mechanism from dislocation to grain boundary (GB) mediated processes occurs when the average grain size is reduced to a critical value [7,8]. In addition to the average grain size, the distribution of grain sizes may also play a crucial role in plastic deformation as the contributions from dislocation- and GB-related motions in large grains could be quite different from those in small grains. Existing studies on the effects of grain size distribution upon deformation mechanism transition have been predominantly based on the studies of single-phase nanocrystalline metals [9]. Little knowledge, if any, has been gained about the mechanical transition in nanoscale metallic multilayers and it is yet clear whether deformation mechanism transition appears in nanoscale multilayer layers if the grain sizes in alternative layers are considerably different. To address this issue, bi-metallic nanoscale multilayers with unequal grain sizes in individual layers would be an interesting system to explore. The mechanism transition, if proven true, could improve our understanding of the deformation behavior of nano-multilayers and enrich the list of plastic deformation mechanisms for nanoscale composite systems.

The primary aim of the present study was to evaluate the deformation behavior, microstructure and possible mechanism transition of unequal grained metallic nano-multilayers. The synthesis of nanoscale Cu/β-Ta multilayers with unequal grain sizes was firstly reported. Subsequently, to distinguish the controlling mechanisms of nanoscaled metallic materials [10–16], the hardness and strain rate sensitivity were determined by conducting nanoindentation testing of the fabricated Cu/Ta multilayers. Enhanced strain rate sensitivity at relatively low strain rates was observed, and its significance in the mechanism transition of nano-multilayers was discussed.

2. Experimental details

Cu/Ta multilayers were deposited on single crystalline Si (1 1 1) substrate using a *d.c.* magnetron sputtering system under an argon pressure of 0.3 Pa at room temperature, with deposition rate fixed at 0.239 nm/s for Cu and 0.177 nm/s for Ta. The nominal individual layer thickness is 30 nm, and the total thickness of a multilayer is 1 μm. The microstructure of the as-deposited Cu/Ta multilayer was examined with both X-ray diffraction (XRD) and transmission

* Corresponding author. Tel.: +86 29 82663869; fax: +86 29 82663453.
E-mail address: wangfei@mail.xjtu.edu.cn (F. Wang).

0921-5093/$ – see front matter © 2011 Elsevier B.V. All rights reserved.
doi:10.1016/j.msea.2011.04.009

electron microscope (TEM). XRD was carried out on a PANalytical's X'Pert Pro X-ray Materials Research Diffractometer using Cu kα radiation at an acceleration voltage of 45 kV. A Philips CM201 TEM operated at 200 kV was used to determine the grain size distribution and identify the deformation mechanisms in the multilayers.

Hardness tests were conducted using MTS Nanoindenter XP® system (MTS, Inc) under Continuous Stiffness Measurement (CSM) mode over a range of loading strain rates, from 10^{-1} s^{-1} to 10^{-5} s^{-1}. The tip of indenter is a Berkovich diamond indenter with a nominal tip radius of curvature of around 50 nm. Whilst the maximum indentation depth was set as ~500 m, the average hardness was obtained at an indentation depth ranging from 50 to 150 nm, which is less than about one-seventh of the film thickness, in order to eliminate the substrate effects. Thermal drift correction was applied to correct drift effects in the nanoindentation tests, with data obtained when the drift rate exceeded 0.03 nm/s discarded. At each loading strain rate, at least 10 effective sets of test data were used for subsequent analysis.

3. Results

3.1. Microstructure

The cross-sectional TEM image shown in Fig. 1(a) revealed that the Cu/Ta multilayers have the same individual thickness of ~30 nm. XRD analysis (inset of Fig. 1(a)) showed that the Cu layer has a strong (1 1 1) peak with face centered cubic (fcc) structure, whilst the Ta layer exhibits a tetragonal structure (β-Ta) with a stronger (0 0 2) peak (33.4°) and a weaker (0 0 4) peak (70.5°). High resolution TEM (HRTEM) examinations showed that the plane spacing of the inclined lines in Fig. 1(b) is 0.207 nm in Cu layers and 0.264 nm in β-Ta layers. Consistent with the strongest peaks in Cu and β-Ta layers revealed by XRD analysis of Fig. 1(a), these fringes can be related to (1 1 1) Cu (d = 0.208 nm) and (0 0 2) β-Ta (d = 0.266 nm).

Subsequently, upon checking the in-plane thinning area of the multilayers, we successfully identified a few representative zones for both Cu (Fig. 2(a)) and Ta layers (Fig. 2(b)). Quantitative analysis of the plane-view grain size distribution indicated that the average and peak grain sizes are about 28 nm and 26 nm for Cu layers and 9.5 nm and 10 nm for Ta layers, respectively. In addition, the out-of-plane distributions of grain size for both Cu and Ta layers were similar to the plane-view ones, suggesting that the grains in these layers are equiaxed.

The HRTEM images presented in Fig. 3(a)–(c) shows in more detail the microstructure of the deformed Cu layer, with twins and dislocations near the grain boundary clearly observed. In contrast, no detectable dislocation and twin in the deformed β-Ta layer of Fig. 3(d) could be seen.

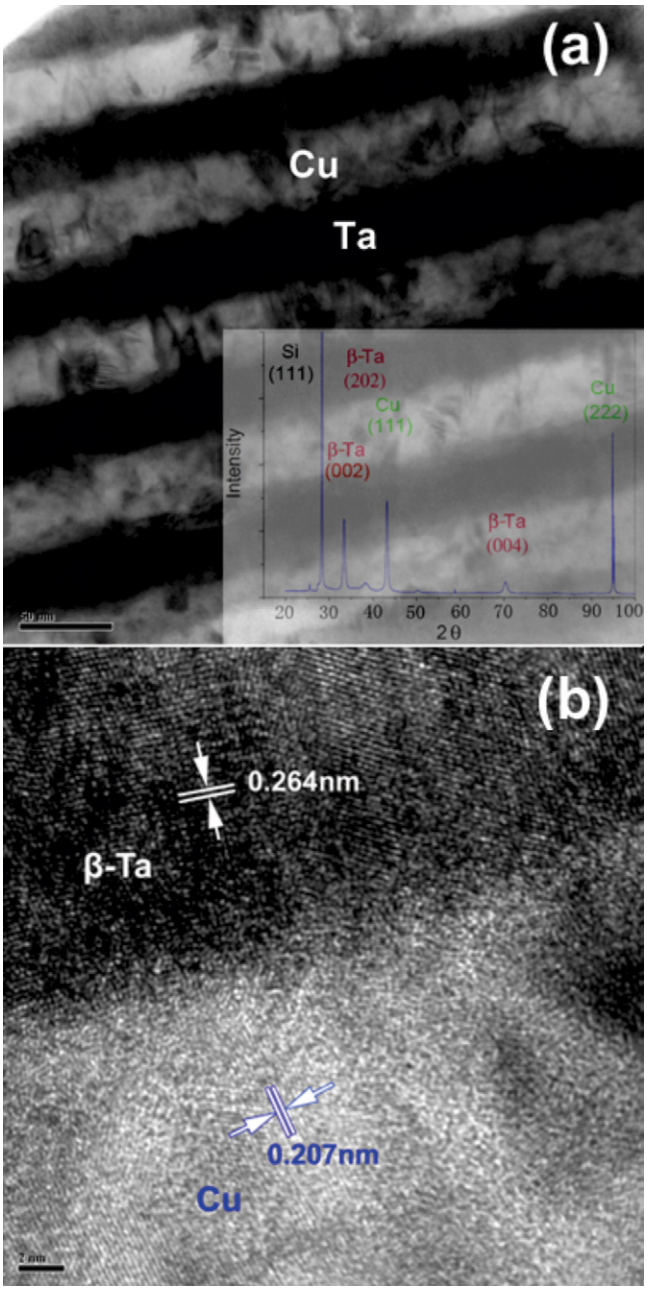

Fig. 1. (a) Bright-field TEM cross-sectional image of 30 nm Cu/Ta multilayer. Inset shows XRD profile of as-deposited multilayer; Cu has fcc structure and Ta has tetragonal structure. (b) HRTEM cross-sectional image of Cu/Ta interlayer.

3.2. Mechanical properties

Fig. 4(a) plots the indentation depth as a function of indentation load for selected strain rates at room temperature. The curves exhibit an experimentally detectable discrepancy, as a higher indentation load is required to reach the same displacement at a larger strain rate. This observation is consistent with previous reports on nanocrystalline metals [17,18], suggesting that the present Cu/Ta multilayers have a positive strain rate sensitivity of stress.

To explore further the strain rate dependent behavior of Cu/Ta multilayers, Fig. 4(b) presents the typical double logarithmic hardness versus loading strain rate curves. A pronounced strain rate dependence of hardness is observed: the hardness increased rapidly from about 1 GPa to 8 GPa as the strain rate was increased from 10^{-5} to 10^{-1} s^{-1}. The strain rate sensitivity m was determined by [17]:

$$m = \frac{\partial \log H}{\partial \log \dot{\varepsilon}} \quad (1)$$

where H and $\dot{\varepsilon}$ are the hardness of the multilayer and the corresponding loading strain rate, respectively. In the strain rate range considered in the present study, the double logarithmic curves of Fig. 4(b) exhibit two distinct linear regimes with m = 0.091 at $\dot{\varepsilon} > 10^{-3}\,s^{-1}$ and 0.286 at $\dot{\varepsilon} < 10^{-3}\,s^{-1}$.

It should be noted that the generated stress state underneath indenter is highly heterogeneous [19] which is very different than those occurring in tensile test. Unlike tensile test, the deformed volume underneath the indenter is continually expanding to the area previously un-deformed. Therefore, in general, the strain rate of

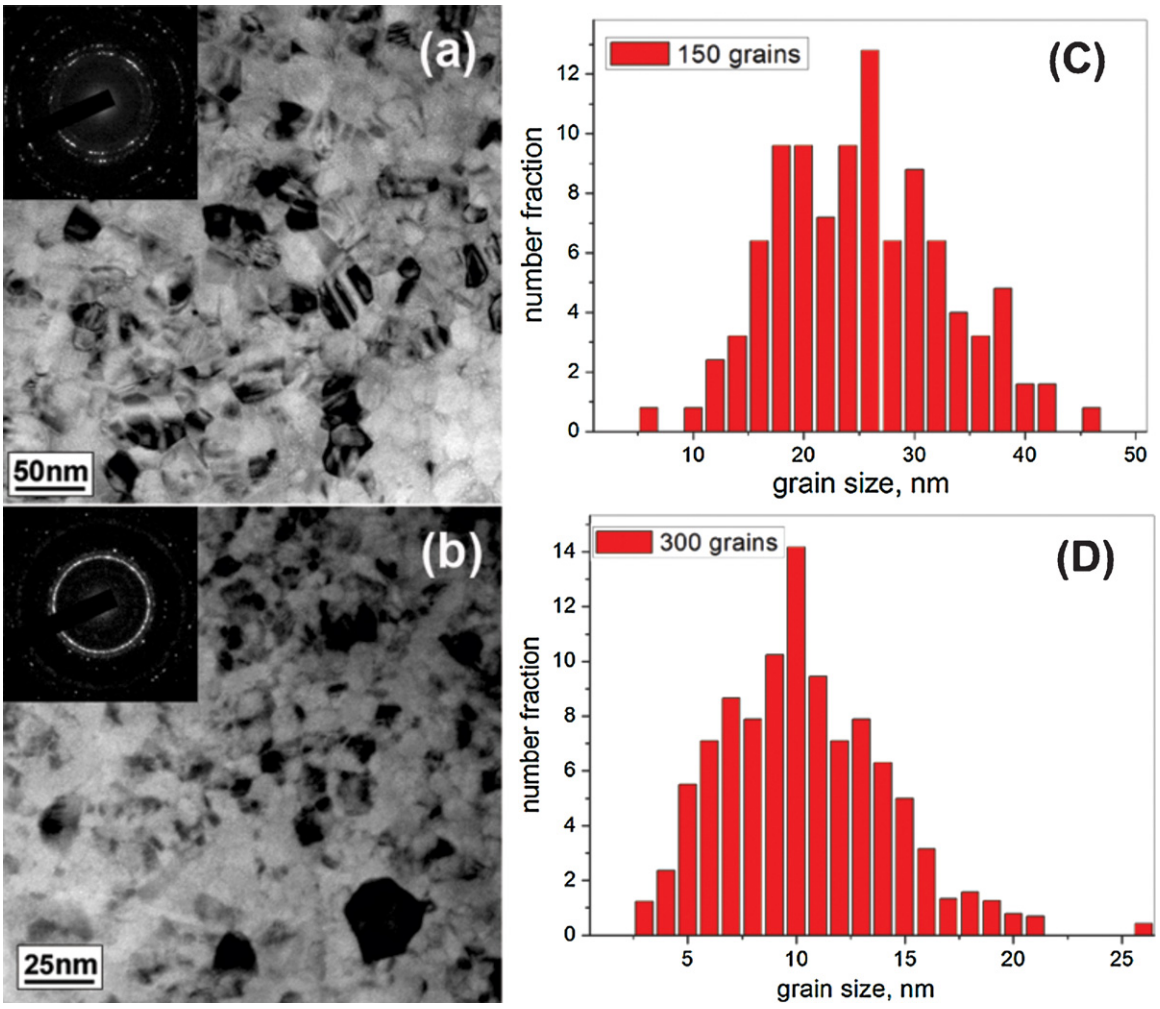

Fig. 2. In-plane TEM images of (a) Cu layer and (b) Ta layer, and corresponding grain size distribution of (c) Cu layer and (d) Ta layer.

indentation test is defined as the ratio of instantaneous penetration depth rate over instantaneous penetration depth for geometrically similar indenter [20], e.g., Berkovich indenter used in present study. Whilst the definition of the strain rate of indentation is deduced from heterogeneous stress state which differs from tensile test, numerous studies indicated that both the magnitude and the variation trends of mechanical parameters, i.e., hardness and strain rate sensitivity, derived from indentation test are comparable to those derived from tensile test [7,17,21–23]. Therefore, Eq. (1) could be used to determine the strain rate sensitivity from constant indentation strain rate tests.

It has been established that the β-Ta phase was unstable with a negative m value, and phase transformation occurred in 9 nm grained β-Ta under nanoindentation [24]. For the present Cu/β-Ta multilayers, the variation of hardness from ~8 GPa to ~1 GPa should mainly be attributed to β-Ta, since the hardness of 28 nm grained Cu could only reach ~2 GPa [22] whereas that of 9 nm grained β-Ta could reach as high as ~16 GPa [24]. This observation indicates that the β-Ta layer had a positive m value in the present Cu/β-Ta multilayers.

4. Discussion

For nanocrystalline metallic materials, it is widely accepted that the dominant deformation mechanism will change from dislocation-mediated to GB-mediated process when the grain size is reduced to less than a critical value. Such mechanism transition is in general associated with either an elevation or reduction of the strain rate sensitivity m, and hence m has important implications in understanding the deformation mechanisms of nanocrystalline metals [10,11,14–17,23]. Specifically, a large m is expected when GB-mediated processes dominate the plastic deformation whereas, in contrast, m would decrease when dislocation-mediated activities prevail [10,12,13]. Therefore, the observed sudden increase of m as the strain rate was reduced to less than $10^{-3}\,s^{-1}$ (Fig. 4(b)) suggests that the transition of deformation mechanisms occurred in the Cu/β-Ta multilayers.

The high strain rate sensitivity of a nanocrystalline metal is related to the enhanced interaction between dislocations and GBs. Extensive MD (molecular dynamics) simulations have demonstrated that dislocations in Nanocrystalline metals could be emitted from the GBs and eventually absorbed by GBs on the opposing side [8]. Recently, a study indicated that dislocation absorption by GBs could be enhanced significantly by varying the strain rate and grain size. The absorption process can be described by a parameter termed as the probability of a dislocation absorbed by GB, as [25]:

$$P_{\mathrm{dis}} = [1 - (1 - e^{M})^{N}]^{J} \tag{2}$$

where N is the number of attempted jumps by dislocation core atoms to the GB during an average time absorption, J is the total number of atoms on the dislocation core jumping into the GB, and M is a mobility factor. As the magnitude of N is inversely proportional to strain rate and grain size, the P_{dis} is highly sensitive to

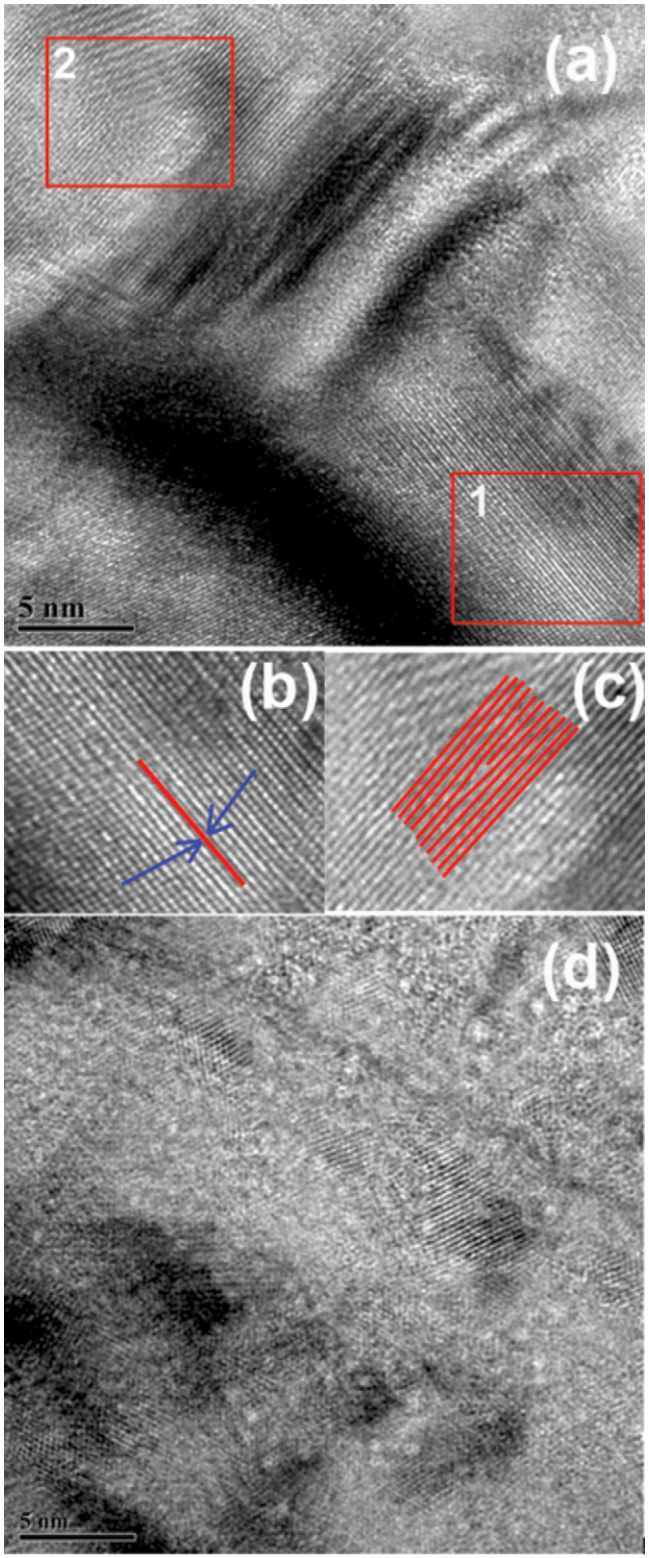

Fig. 3. (a) Low-magnification in-plane TEM image of Cu layer; (b) magnified image of zone "1", showing a twin near GB conjunction; (c) magnified image of zone "2", showing the existence of dislocation in Cu grain; (d) HRTEM cross-sectional image of β-Ta layer.

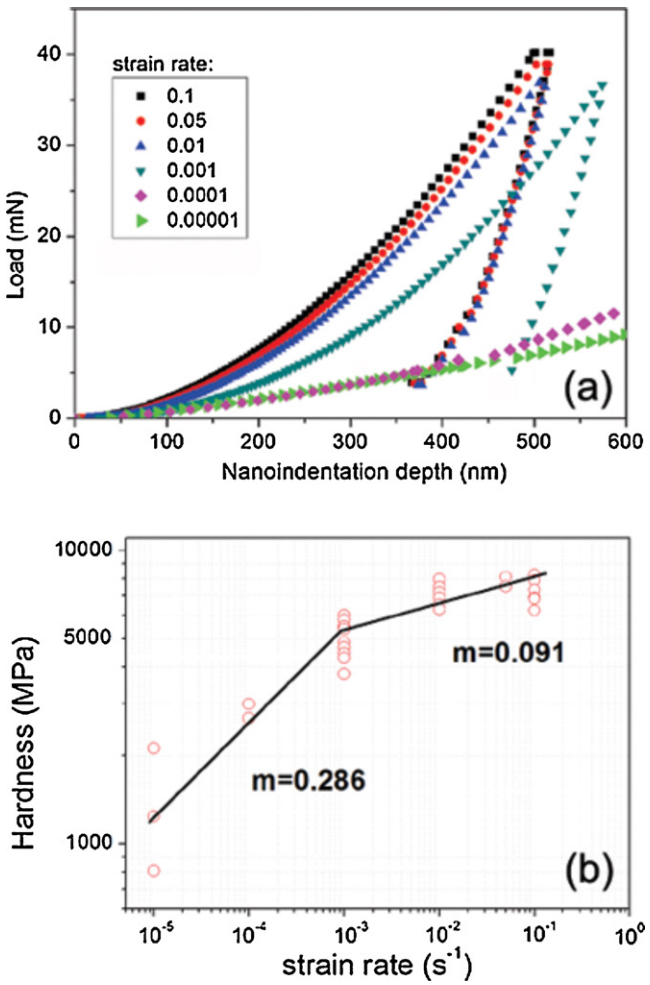

Fig. 4. (a) Load plotted as a function of nanoindentation depth for selected strain rates ranging from 10^{-1} s^{-1} to 10^{-5} s^{-1}; (b) hardness plotted as a function of strain rate.

strain rate and grain size [25]. With these pictures in mind, the value of m and its transition as observed in Fig. 4(b) could be interpreted by considering the effects of both strain rate and grain size on m of the present Cu/Ta multilayers.

4.1. Effect of strain rate

According to the analysis of Carlton [25], a faster strain rate results in a smaller P_{dis} whereas a larger P_{dis} corresponds to a slower strain rate. We consider first the effects of strain rate on local grain structure and stress state. Given that dislocations are generally nucleated from ledges located in GBs and the nucleation process can effectively release the local stress concentration [26,27], the GB structure could be more homogenized by emitting dislocations from GBs. Therefore, there should be less ledges and reduced local stress concentrations in nanoscale grains. With these pictures in mind, then, the strain rate dependent microstructure evolution might be described by the following scenario.

When nanoscale grains deform at a faster strain rate with a smaller P_{dis}, more dislocations emit from the ledges to impinge on opposite GBs per unit time. Compared with the case of a slower strain rate, less time was left for the absorption process of the emitted dislocations to complete, and heavier dislocation–storage at the opposite GBs was built. The higher internal stresses generated from the repeated emit–absorb process will then effectively obstruct the processes of nucleation and emission of new

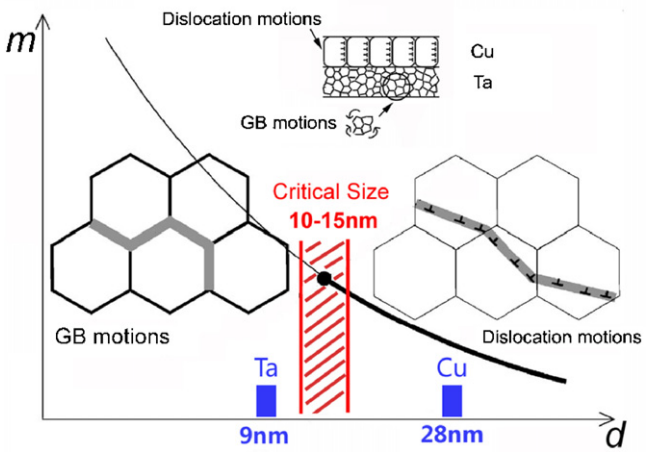

Fig. 5. Schematic illustration of strain rate sensitivity m as a function of grain size d.

dislocations from the GB, leaving more ledges at the GB source. At a slower strain rate with a larger P_{dis}, the absorption process is relatively easy to operate, resulting in lighter dislocation storage and lower internal back stresses and hence, more homogenous grain structures. Consequently, the less ledges and lower internal stresses at slow strain rates may effectively enhance the GB motion compatibility between neighboring grains, resulting in a higher m attributed from both the Cu and Ta layers.

4.2. Effect of grain size

Along strain rate, grain size is another important parameter governing the plastic deformation of nanocrystalline metals. For Cu, the critical value of grain size below which GB-mediated mechanism dominates the plastic deformation is 10–15 nm [28], which is much smaller than the grain size found in the present Cu layers. Moreover, the size of in-plane grains and the presence of twins and dislocations shown separately in Figs. 2(a) and 3(a)–(c) indicate that the deformation of the Cu layer should be dominated by dislocation-mediated mechanisms as illustrated in Fig. 5.

In contrast to Cu, the critical grain size of Ta is still less understood as only a few studies concerned the deformation mechanism of nanocrystalline Ta [19,29]. Noting that the total volume fraction of GBs and triple junctions in a ~10 nm grained nanocrystalline metal could reach as high as 25%, the GB motions in the present 9 nm grained β-Ta layer should have more mobility than those in the 28 nm grained Cu layer. Pan et al. [30] revealed that the breakdown of the Hall–Petch relation occurred in Ta with grain sizes ranging from 4 to 13 nm, which involved grain rotation, GB sliding and dislocation motions, and a strain rate sensitivity of ~0.14 in 6.5 nm grained Ta was obtained. However, as this value is still 3 times smaller than that expected from GB sliding ($m = 0.5$ [31]), the dominant mechanism of the 9 nm grained Ta layer is most likely to be GB motions accommodated by dislocation-mediated processes; see Fig. 5.

To evaluate the effects of grain size, we need to consider the *dislocation-mean-free-path* (l) defined as the distance traveled by a dislocation segment from nucleation source to where it is finally stored by interaction with GB. The representative l in the 9 nm Ta layer should be much smaller than that in the 28 nm grained Cu layer as l is proportional to grain size. Hence, the emitted dislocations can reach the opposite GBs more easily in the 9 nm Ta layer, resulting in the increase of P_{dis}.

The random grain orientations (Fig. 3(d)) and the relatively small grain size (9 nm) of β-Ta layers are beneficial for uncorrelated atom shuffling and stress-assisted diffusion [32]. Meanwhile, the large percentage of GB atoms/total atoms in the β-Ta layers favors the GB-related mechanisms, leading to a higher m.

In view of the discussion above for nanoscaled Cu/β-Ta multilayers, the variation of m shown in Fig. 4 may be interpreted by separating the strain rate into two regimes, and the scenarios underlying the sudden change of strain rate sensitivity may be visualized, as illustrated in the following sub-section.

4.3. Deformation mechanisms of Cu/Ta multilayers under nanoindentation

In the high strain rate ($>10^{-3}\,s^{-1}$) regime, the large stresses enable easier nucleation and emission of dislocations from GBs in both Cu and Ta layers, and the dislocation-mediated mechanism dominates the plastic deformation of the multilayer. Since dislocations are typically formed in the softer layer within a multilayer having different hardness in alternating layers [5,6], upon indentation loading plastic yielding should initially occur in Cu grains in the present Cu/Ta multilayer. The nucleation and emission of dislocations in 9 nm grained β-Ta will require much higher stresses than the 28 nm grained Cu and hence serve only as subordinate processes.

At high strain rates, the more ledges available and large internal stresses generated may effectively impede the GB motion compatibility as discussed in Section 4.1, resulting in smaller m values. In addition, given that the grain size is another crucial parameter, the shorter l in 9 nm grained Ta layers leaves less time for dislocation absorption than that in 28 nm grained Cu layers, leading to smaller P_{dis} and m. The plastic deformation of Cu/Ta multilayers exhibits therefore relatively less rate sensitivity in the high strain rate regime, as observed in the present experimental study.

As the strain rate is reduced to below $10^{-3}\,s^{-1}$ (i.e., low strain rate regime), the relatively small internal stresses may not be sufficient for dislocation nucleation and emission at GBs and, as a result, GB deformation in β-Ta may increasingly become preferable. In this regime, the measured value of m (0.286) is close to that (0.5) due to GB sliding, indicating that the contribution of GB-mediated processes is significantly enhanced. This may be attributed to the fact that, in addition to the relatively sufficient time for dislocation absorption, the shorter l traveled by dislocation segments can concurrently increase the P_{dis} and hence enlarge the magnitude of m in 9 nm grained β-Ta layers. Note that the value of m (0.286) for $\dot{\varepsilon} < 10^{-3}\,s^{-1}$ is about 2 and 3 times higher than the maximum m reported previously for ultra-fine grained Cu [33] and nanocrystalline Cu [11], respectively. This suggests that the increase of m as the strain rate in reduced to less than $10^{-3}\,s^{-1}$ is mainly attributable to the β-Ta layers, not the Cu layers.

On the other hand, the existence of disorientations in β-Ta layers as shown in Fig. 3d could enable the GB region to easily deform via diffusion and sliding. The deformation of β-Ta layers would therefore dominate the plastic deformation of the multilayer as well as its strain rate sensitivity m, with dislocation-mediated processes in Cu layers acting as the subordinate mechanism.

It should be pointed out that the effects of interfaces on m have not been considered here, and it would be difficult at this stage to determine the actual contribution of each layer to the total plastic deformation in each strain rate regime. More thorough examinations concerning the effects of grain size, layer thickness and interface properties on the plastic deformation of nanoscaled metallic multilayers are needed.

5. Conclusion

Nanoscaled Cu/Ta multilayers having equal individual layer thickness but distinct grain sizes in alternative layers were

successfully fabricated and their deformation behaviors under nanoindentation characterized, with focus placed on strain rate sensitivity and transition of deformation mechanisms. By evaluating the hardness at selected strain rates, the transition of strain rate sensitivity at strain rate as high as $10^{-3}\ s^{-1}$ was observed for the first time. The appearance of the transition was interpreted as competitions between dislocation-mediated and GB-mediated mechanisms in Cu and Ta layers as the strain rate is varied. At higher strain rates ($>10^{-3}\ s^{-1}$), plastic deformation of the Cu/Ta multilayer is dominated by dislocation-mediated mechanisms in Cu. At low strain rates ($<10^{-3}\ s^{-1}$), the GB-mediated mechanisms in Ta dominate, increasing significantly the strain rate sensitivity of the Cu/Ta multilayers.

Acknowledgements

This work was supported by the National Basic Research Program of China (2011CB610306, 2010CB631002), the National Natural Science Foundation of China (50701034, 10825210), the National 111 Project of China (B06024), the Program for New Century Excellent Talents in University (NCET-07-0665) and the Fundamental Research Funds for the Central Universities.

References

[1] N.J.M. Carvalho, J.T.M. De Hosson, Acta Mater. 54 (2006) 1857–1862.
[2] A. Misra, J.P. Hirth, R.G. Hoagland, Acta Mater. 53 (2005) 4817–4824.
[3] N.A. Mara, T. Tamayo, A.V. Sergueeva, X. Zhang, A. Misra, A.K. Mukherjee, Thin Solid Films 515 (2007) 3241–3245.
[4] B.C. Kang, H.Y. Kim, O.Y. Kwon, S.H. Hong, Scr. Mater. 57 (2007) 703–706.
[5] L. Fang, L.H. Friedman, Acta Mater. 55 (2007) 1505–1514.
[6] M.A. Phillips, B.M. Clemens, W.D. Nix, Acta Mater. 51 (2003) 3157–3170.
[7] M. Dao, L. Lu, R.J. Asaro, J.T.M. De Hosson, E. Ma, Acta Mater. 55 (2007) 4041–4065.
[8] D. Wolf, V. Yamakov, S.R. Phillpot, A. Mukherjee, H. Gleiter, Acta Mater. 53 (2005) 1–40.
[9] B. Zhu, R.J. Asaro, P. Krysl, K. Zhang, J.R. Weertman, Acta Mater. 54 (2006) 3307–3320.
[10] Y.J. Wei, A.F. Bower, H.J. Gao, Acta Mater. 56 (2008) 1741–1752.
[11] Z.H. Jiang, X.L. Liu, G.Y. Li, Q. Jiang, J.S. Lian, Appl. Phys. Lett. 88 (2006) 143115.
[12] Z.H. Jiang, H.Z. Zhang, C.D. Gu, Q. Jiang, J.S. Lian, J. Appl. Phys. 104 (2008) 053505.
[13] G.Y. Wang, Z.H. Jiang, Q. Jiang, J.S. Lian, J. Appl. Phys. 104 (2008) 084305.
[14] P. Huang, F. Wang, M. Xu, K.W. Xu, T.J. Lu, Acta Mater. 58 (2010) 5196–5205.
[15] F. Wang, P. Huang, K.W. Xu, Appl. Phys. Lett. 90 (2007) 161921.
[16] F. Wang, P. Huang, K. Xu, Surf. Coat. Technol. 201 (2007) 5216–5218.
[17] J.R. Trelewicz, C.A. Schuh, Acta Mater. 55 (2007) 5948–5958.
[18] R. Schwaiger, B. Moser, M. Dao, N. Chollacoop, S. Suresh, Acta Mater. 51 (2003) 5159–5172.
[19] W.A. Soer, K.E. Aifantis, J.Th.M. De Hosson, Acta Mater. 53 (2005) 4665–4676.
[20] B.N. Lucas, W.C. Oliver, Metal. Mater. Trans. 30A (1999) 601–610.
[21] R. Scheaiger, B. Moser, M. Dao, N. Chollacoop, S. Suresh, Acta Mater. 51 (2003) 5159–5172.
[22] J. Chen, L. Lu, K. Lu, Scr. Mater. 54 (2006) 1913–1918.
[23] R.J. Asaro, S. Suresh, Acta Mater. 53 (2005) 3369–3382.
[24] Y.M. Wang, A.M. Hodge, P.M. Bythrow, T.W. Barbee, A.V. Hamza, Appl. Phys. Lett. 89 (2006) 081903.
[25] C.E. Carlton, P.J. Ferreira, Acta Mater. 55 (2007) 3749–3756.
[26] H. Van Swygenhoven, Mater. Sci. Eng. A 483 (2008) 33–39.
[27] H. Van Swygenhoven, J.R. Weertman, Mater. Today 9 (2006) 24–31.
[28] J. Schiotz, K.W. Jacobsen, Science 301 (2003) 1357–1359.
[29] Z.H. Cao, P.Y. Li, H.M. Lu, Y.L. Huang, Y.C. Zhou, X.K. Meng, Scr. Mater. 60 (2009) 415–418.
[30] Z.L. Pan, Y.L. Li, Q. Wei, Acta Mater. 56 (2008) 3470–3480.
[31] H. Luthy, R.A. White, O.D. Sherby, Mater. Sci. Eng. 39 (1979) 211–216.
[32] H. Van Swygenhoven, P.A. Derlet, Phys. Rev. B 64 (2001) 224105.
[33] R.Z. Valiev, I.V. Alexandrov, Y.T. Zhu, T.C. Lowe, J. Mater. Res. 17 (2002) 5–8.